



HAL
open science

Geometry and topology in 3D polarization

Miguel Alonso

► **To cite this version:**

Miguel Alonso. Geometry and topology in 3D polarization. SPIE Optical Engineering + Applications,, Aug 2023, San Diego, United States. 10.1117/12.2684647 . hal-04280485

HAL Id: hal-04280485

<https://hal.science/hal-04280485>

Submitted on 11 Nov 2023

HAL is a multi-disciplinary open access archive for the deposit and dissemination of scientific research documents, whether they are published or not. The documents may come from teaching and research institutions in France or abroad, or from public or private research centers.

L'archive ouverte pluridisciplinaire **HAL**, est destinée au dépôt et à la diffusion de documents scientifiques de niveau recherche, publiés ou non, émanant des établissements d'enseignement et de recherche français ou étrangers, des laboratoires publics ou privés.

Geometry and Topology in 3D polarization

Miguel A. Alonso^{*a,b}

^aAix Marseille Univ, CNRS, Centrale Marseille, Institut Fresnel, Marseille, France;

^bThe Institute of Optics, University of Rochester, Rochester NY 14627, U.S.A.

ABSTRACT

This presentation will give an overview of the local description of polarization for nonparaxial light, for which all three Cartesian components of the electric field are significant. The polarization of light at each point is characterized by a three-component complex vector in the case of full polarization and by a 3×3 polarization matrix for partial polarization. Standard concepts in paraxial polarization such as the degree of polarization, the Stokes parameters, and the Poincaré sphere, have generalizations for nonparaxial light that are not unique and/or not trivial. Particular emphasis is placed on geometric interpretations and their similarities and differences with those for the paraxial regime, as well as topological features. An application of this formalism in super-resolution microscopy is presented.

Keywords: Polarization, geometry, topology, imaging, fluorescence microscopy.

1. INTRODUCTION

The two Maxwell equations involving divergences imply that, in media that are transparent and isotropic, electromagnetic waves are transverse. However, only for waves with a well-defined direction of propagation, such as plane waves or paraxial beams, do these conditions imply that a given component of the field is zero or negligible. It is for these conditions that the standard theory of polarization was formulated. Nevertheless, more and more applications emerge involving light propagation that does not meet these assumptions. These include the field of plasmonics, evanescent waves, or interactions of matter with strongly focused light. In situations such as high numerical-aperture microscopy, the standard polarization formalism can be used when working in the pupil (or Fourier) plane, but not when considering the interaction of the field with the sample.

For all these applications in which all three components of the electric field vector can play a role, the standard formalism of polarization must be extended. Many authors have proposed extensions to the nonparaxial regime of concepts such as the degree of polarization or the Poincaré sphere. Here I give a short overview of some of these results. A more detailed account is given in Ref. 1. The cases of full and partial polarization are discussed in Sections 2 and 3, respectively. In both cases, the section begins with a summary of key concepts for paraxial (2D) polarization and then continues with a discussion of the extension of these concepts to nonparaxial (3D) polarization. The last part of Section 3 gives a very brief discussion of how some of these concepts are useful in combination with imaging techniques.

2. FULLY POLARIZED MONOCHROMATIC FIELDS

2.1 2D polarization

For a fully polarized monochromatic paraxial field traveling in the positive z direction, only the x and y components of the electric field vector are significant. The field traces in time an ellipse within the (E_x, E_y) plane. It can be then described locally in terms of a global phase for the oscillations, a magnitude factor, and its polarization, the latter consisting of the purely geometric aspects of the oscillation including the ellipticity, orientation and handedness. As shown in Fig. 1(a), ellipticity can be quantified by using the angle θ subtended by the minor axis over a distance from the major semi-axis. For $\theta = 0$ the ellipse reduces to a line, while for $|\theta| = \pi/2$ it gives a circle. Further, the handedness of the ellipse can be encoded in the sign of θ . The orientation of the ellipse, on the other hand, can be encoded by the angle $\phi/2$, the factor of one half ensuring a periodicity of 2π . The ranges of variation for these two angles suggest that they can be used as latitude and longitude coordinates over a sphere, known as the Poincaré sphere. That is, polarization can be represented as a point on the surface of a unit sphere.

*miguel.alonso@fresnel.fr.

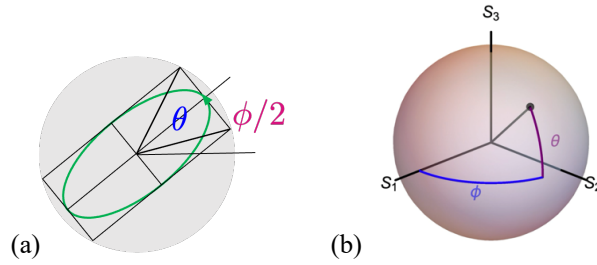


Figure 1. 2D full polarization. (a) Definition of the angles that define the ellipticity, handedness and orientation of the ellipse. (b) Definition of the Poincaré sphere, whose spherical coordinates are the angles in (a).

The Poincaré sphere representation reflects the geometry intrinsic to the space of polarization states. For example, the effect of the passage of light through a transparent birefringent medium corresponds to a rotation of the Poincaré sphere by an angle equal to the retardance, around an axis defined by the medium's eigenpolarizations. Also, it is well known that a (discrete or continuous) sequence of polarization transformations imparts a phase, known as geometric phase, that is separate from the dynamic phase due to the accumulation of optical path length. The geometric phase is equal to one half of the solid angle enclosed by the path over the Poincaré sphere describing the series of polarization transformations. Perhaps the only aspect of the Poincaré sphere representation that could be regarded as a mild drawback is the fact that its axes do not correspond to those in physical space but to the Stokes parameters described later.

2.2 3D polarization

Beyond the paraxial regime, the electric field still traces an ellipse over time, but this ellipse is constrained to a plane whose orientation must also be specified. Therefore, four quantities are needed to describe polarization instead of two. For example, two angles can be used to define the plane of oscillation, and two more to describe the ellipticity and orientation within this plane. It is natural to wonder if there is a counterpart of the Poincaré sphere to represent nonparaxial polarization, and whether such representation presents analogous properties to those of the Poincaré sphere. In this section we consider the option of an easy-to-visualize sphere in 3D, as in the paraxial regime. It turns out that several options exist that capture the intrinsic geometry of nonparaxial polarization ellipses. Due to the number of parameters involved, though, these descriptions require the prescription of two (indistinguishable) points instead of just one. We now describe three of them, which share many common traits. In particular, they all have the desirable property of having axes associated with the physical directions x, y, z instead of more abstract directions as in the paraxial case.

Before entering into details that are specific to each of the three representations, let us describe the general aspects that these constructions share. Consider an ellipse with arbitrary 3D orientation, ellipticity and handedness, as shown in Fig. 2(a). If the complex field is normalized to unity, this ellipse is geometrically normalized in the sense that it can be inscribed in a rectangle whose diagonals have length two. That is, this rectangle itself can be inscribed in a unit disk, and this disk can be fit within the unit sphere, as the figure shows. The goal is to represent this ellipse in terms of two points over the surface of the sphere. To distinguish the handedness of the field oscillation along the ellipse, the two points are constrained to one of the two hemispheres defined by the intersection of the sphere and the plane containing the ellipse. The choice of the hemisphere follows the right-hand rule. The direction of the ellipse's major axis is indicated by choosing the two points to be along a line parallel to this axis, and the normal to the ellipse corresponds to the vector bisecting the two points. This means that both points are along a great semicircle corresponding to the intersection with the hemisphere of a plane normal to the plane of the ellipse and that contains the ellipse's major axis, and at equal angles with respect to the ellipse's normal. Finally, the ellipticity must be encoded in the separation of the two points, with the two limiting cases: the two points must coincide when the ellipse is circular, since the major axis is not uniquely defined; at the opposite limit, the two points must be antipodal when the ellipse is linear, since the plane containing the ellipse is not uniquely defined.

The first two-point representation of nonparaxial polarization is based on Majorana's representation for spin systems [2]. Its application to 3D polarization was suggested by Penrose [3] and formalized by Hannay [4]. In this representation, the two points correspond to the two points of view from which the ellipse projects onto a circle, as shown in Fig. 2(b).

The second representation was proposed recently [5], with the motivation of presenting the same link to geometric phase as the Poincaré sphere in the paraxial regime: the geometric phase accumulated after a sequence of polarization changes

that finishes at the initial polarization state corresponds to one half of the enclosed solid angle, in this case by two points. Because it incorporates aspects from the Poincaré and Majorana representations, this second representation was referred to as the “Poincarana” representation. As shown in Fig. 2(c), the midpoint (or centroid) of the two points equals the local spin density, which is a vector normal to the ellipse whose length is proportional to the area of the ellipse, such that it takes a maximum magnitude of unity when the ellipse is a circle.

The third representation was defined [1] to be linked with the statistical description of nonparaxial polarization, so that for random superpositions of plane waves the statistics of the two points are uncorrelated. As illustrated in Fig.2(d), the two points are the intersections with the sphere to normal lines to the plane containing the ellipse, emerging from the centers of circles inscribed in the same rectangle as the ellipse.

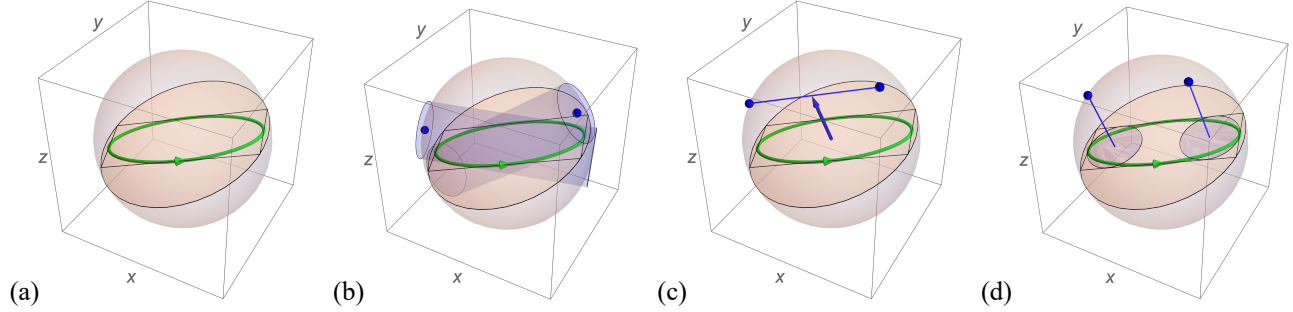


Figure 2. Representation of nonparaxial polarization ellipses (green) with two points (small blue spheres) over a unit sphere. (a) The polarization ellipse can have an arbitrary ellipticity and orientation in 3D. It is normalized such that it is inscribed in a rectangle that itself is inscribed in a unit circle. This circle limits the hemisphere where the two points are contained, in order to encode handedness following the right-hand rule. (b) Hannay-Majorana representation, where the two points are chosen as the directions from which the ellipse projects onto a circle or, equivalently, as the intersections of the hemisphere with the axes of each of two circular cylinders that contain the ellipse. (c) Poincarana representation, where the two points are the intersections of the hemisphere with a straight line parallel to the ellipse’s major axis that contains also the tip of the spin density vector (blue arrow). (d) Statistically motivated representation, where the points are chosen as the normal projections onto the hemisphere of the centers of two circles that fit at the ends of the rectangle containing the ellipse.

2.3 Topology

A field’s spatial distribution of polarization, whether it is 2D or 3D, can lead to interesting topological structures such as skyrmions, which correspond to distributions that span all possible states in a (N-)spherical parameter space. A first example of this is that of the so-called full Poincaré beams [6], which at any transverse plane span all the surface of the Poincaré sphere according to a stereographical mapping. Many other implementations exist, where the spherical space is not necessarily the Poincaré sphere but the field direction at a given instant [7]. We recently proposed a “full Poincarana field” that spans the 4D space of nonparaxial polarization [8].

3. PARTIALLY POLARIZED QUASIMONOCROMATIC FIELDS

3.1 2D polarization

When light is not perfectly monochromatic, the electric field traces a far more complex curve than an ellipse. Typical measurements can only access the second-order statistics of such oscillation since the typical integration times of the detectors are far longer than both the typical optical cycle and the characteristic times of fluctuation of the path. These second-order statistics are described mathematically by the polarization matrix

$$\mathbf{\Gamma}_{2D} = \begin{pmatrix} \langle E_x^* E_x \rangle & \langle E_x^* E_y \rangle \\ \langle E_y^* E_x \rangle & \langle E_y^* E_y \rangle \end{pmatrix} \quad (1)$$

where the angular brackets denote a correlation. This matrix is Hermitian and non-negative definite, and therefore it contains four degrees of freedom. It can be written in terms of four parameters as

$$\mathbf{\Gamma}_{2D} = \frac{1}{2} \begin{pmatrix} S_0 + S_1 & S_2 - iS_3 \\ S_2 + iS_3 & S_0 - S_1 \end{pmatrix} \quad (2)$$

where S_n are the so-called Stokes parameters. In particular, S_0 corresponds to the intensity so it does not describe polarization. This parameter can be used, though, to renormalize the remaining three parameters as $s_n = S_n/S_0$. It turns out that these three normalized parameters are the Cartesian coordinates of the Poincaré sphere, and that any point (s_1, s_2, s_3) in this space is constrained by the non-negativity of the matrix to be on the surface or the interior of the sphere, the surface corresponding to fully polarized light, and the interior to partially polarized light.

3.2 3D Polarization

For nonparaxial light, the path traced by the electric field can not only depart from an ellipse, but it typically is not constrained to a plane. The polarization matrix is now a 3 by 3 Hermitian non-negative matrix given by

$$\mathbf{\Gamma} = \begin{pmatrix} \langle E_x^* E_x \rangle & \langle E_x^* E_y \rangle & \langle E_x^* E_z \rangle \\ \langle E_y^* E_x \rangle & \langle E_y^* E_y \rangle & \langle E_y^* E_z \rangle \\ \langle E_z^* E_x \rangle & \langle E_z^* E_y \rangle & \langle E_z^* E_z \rangle \end{pmatrix} \quad (3)$$

which can also be written in terms of nine real parameters, called here the Stokes-Gell-Mann parameters:

$$\mathbf{\Gamma} = \frac{1}{2} \begin{pmatrix} \frac{2}{3}S_0 + S_{11} + \frac{S_{12}}{\sqrt{3}} & S_{23} - iS_{33} & S_{22} + iS_{32} \\ S_{23} + iS_{33} & \frac{2}{3}S_0 - S_{11} + \frac{S_{12}}{\sqrt{3}} & S_{21} - iS_{31} \\ S_{22} - iS_{32} & S_{21} + iS_{31} & \frac{2}{3}S_0 - 2\frac{S_{12}}{\sqrt{3}} \end{pmatrix} \quad (4)$$

where again S_0 corresponds to the intensity. The other parameters can be normalized as $s_{mn} = (3^{1/2}/2) S_{mn}/S_0$ so that a point in an 8D space $(s_{11}, s_{12}, s_{21}, s_{22}, s_{23}, s_{31}, s_{32}, s_{33})$ is again constrained to the surface or the interior of a unit hypersphere. However, the non-negativity of the polarization matrix actually places much stricter restrictions on these parameters [1], such that only 2.64% of the hypervolume corresponds to physical polarization states. The shape of the inhabitable space in eight dimensions is difficult to visualize, but a study in terms of subspaces is described in Ref. 1.

3.3 A representation in a regular sphere

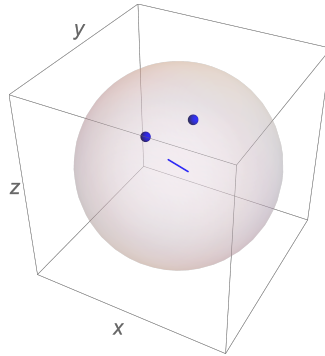


Figure 3. Representation of partial 3D polarization in terms of two points (blue spheres) and a director (blue stick) inside a unit sphere. Like for the Poincarana representation, the centroid of the two points corresponds to the spin density vector. The line joining these points is parallel to the major axis of an ellipsoid characterizing the field's oscillations and the point separation is proportional to the difference of the squares of the two largest semiaxes lengths for this ellipsoid. The director's length is proportional to the difference between the squares of the two smallest semiaxes of the ellipsoid and it is parallel to the direction of the smallest axis. This director is then constrained to be perpendicular to the line joining the two points. In the limit of full polarization, this construction reduces to the Poincarana representation.

It is tempting to propose a representation of partial polarization consisting of a collection of points constrained to the surface and interior of a unit sphere whose axes correspond to the directions of the physical space, hence generalizing one of the representations described in Section 2.2. These points must encode eight degrees of freedom contained in the

Stokes-Gell-Mann parameters. One option proposed in Ref. 1 employs two indistinguishable points constrained to the interior and surface of the sphere, supplemented by a director (a vector or point with a sign ambiguity), which is constrained to be orthogonal to the line joining the two points. In the limit of a fully polarized field the director becomes irrelevant and the two indistinguishable points go to the surface of the sphere and they become the Poincarana points.

3.4 Applications in imaging polarimetry

Both for 2D or 3D polarization the description in terms of Stokes parameters is particularly convenient for experimental work as these parameters are linearly related to measured quantities. We recently proposed imaging polarimetry techniques suitable for objects composed of point-like sources that are sparse enough that their point-spread functions (PSFs) do not overlap. In these techniques, in addition to (2D or 3D) localization of these points, one can retrieve the state of polarization [9,10]. The key is to tailor the PSF by inserting a suitable birefringent mask in the pupil plane of the imaging system. In the case of 2D polarization, this technique has been used for a single-shot measurement of the polarization of the light emerging from each core in a multicore fiber bundle [11]. For 3D polarization, the application we have explored is the determination of the 3D orientation and state of wobble of fluorophores, which can also be localized beyond the diffraction limit by combining this method with super-resolution techniques [12]. Both in the 2D and 3D cases, the measured PSFs are a linear combination of a known set of PSF elements in a basis, whose coefficients are the Stokes parameters we seek to estimate. The goal of the PSF shaping mask is to make the PSF elements as different as possible. For fluorescence microscopy, the statistics of the 3D orientation of the (typically wobbling) fluorophore are described to second order by a matrix analogous to that in Eq. (3), which also describes the fluorescence radiated by this molecule.

ACKNOWLEDGEMENTS

I thank many collaborators in topics related to the one described here, in particular Thomas G. Brown, Sophie Brasselet, Mark Dennis, Konstantin Bliokh, Etienne Brasselet, Hervé Rigneault, Jon Petrucci, Nicole Moore, Anthony Vella, Rodrigo Gutiérrez Cuevas, Luis Alemán Castañeda, Isael Herrera, and David Marco.

I also acknowledge funding from France's Agence Nationale de Recherche (ANR-21-CE24-0014-01).

REFERENCES

- [1] M.A. Alonso, "Geometric descriptions for the polarization for nonparaxial fields: a tutorial", *Adv. Opt. Phot.* **15**, 176-235 (2023).
- [2] E. Majorana, "Atomi orientati in campo magnetico variabile," *Nuovo Cimento* **9**, 43-50 (1932).
- [3] R. Penrose, *The Emperor's New Mind* (Oxford University Press, 1989 349–352).
- [4] J. H. Hannay, "The Majorana representation of polarization, and the berry phase of light," *J. Mod. Opt.* **45**, 1001-1008 (1998).
- [5] K. Y. Bliokh, M. A. Alonso, and M. R. Dennis, "Geometric phases in 2D and 3D polarized fields: geometrical, dynamical, and topological aspects," *Rep. Prog. Phys.* **82**, 122401 (2019).
- [6] A. M. Beckley, T. G. Brown, and M. A. Alonso, "Full Poincaré beams," *Opt. Express* **18**, 10777–10785 (2010).
- [7] R. D. Muelas-Hurtado, K. Volke-Sepulveda, J. L. Ealo, F. Nori, M. A. Alonso, K. Y. Bliokh, and E. Brasselet, "Observation of polarization singularities and topological textures in sound waves," *Phys. Rev. Lett.* **129**, 204301 (2022).
- [8] D. Marco and M. A. Alonso, "Optical fields spanning the 4D space of nonparaxial polarization," arXiv:2212.01366 (2022).
- [9] R. Ramkhalawon, T.G. Brown, and M.A. Alonso, "Imaging the polarization of a light field," *Opt. Express* **21**, 4106-4115 (2013).
- [10] A. Vella and M.A. Alonso, "Optimal birefringence distributions for imaging polarimetry," *Opt. Express* **27**, 36799-36814 (2019).
- [11] S. Sivankutti, E.R. Andresen, G. Bowmans, T.G. Brown, M.A. Alonso, and H. Rigneault, "Single shot polarimetry of multicore fiber," *Opt. Lett.* **41**, 2105-2108 (2016).
- [12] V. Curcio, L.A. Alemán-Castañeda, T.G. Brown, S. Brasselet and M.A. Alonso, "Birefringent Fourier filtering for single molecule Coordinate and Height super-resolution Imaging with Dithering and Orientation," *Nature Comm.* **11**, 5307 (2020).